Diffusion on deterministic and quasirandom models of diffusion-limited aggregates. II. Anisotropic diffusion

Hernan L. Martinez, Juan M. R. Parrondo,* and Katja Lindenberg
Department of Chemistry and Institute for Nonlinear Science, University of California, San Diego, La Jolla, California 92093-0340
(Received 17 February 1993)

In the preceding paper, we discuss the diffusion of a particle on deterministic and quasirandom fractal structures designed to mimic the properties of diffusion-limited aggregates. In this paper we deal with biased transport, that is, transport in the presence of an external field. Our method is based on a renormalization procedure that allows us to calculate the scaling properties relating distance and time as a function of the strength of the external field. We calculate hopping probabilities and mean first-passage times and show how these properties depend on the direction relative to the field and on the branching properties of the model.

PACS number(s): 05.40.+j, 02.50.−r

I. INTRODUCTION

In the preceding paper [1] we noted that the study of transport properties in certain deterministic and quasirandom fractals might serve as a basis for understanding transport in random fractals such as diffusion-limited aggregates (DLA's) [2,3]. We took advantage of the fact that it is possible to construct an exact renormalization scheme for continuous-time random walks [4] on such deterministic and quasirandom structures. The renormalization scheme is established between the probability densities of waiting times on an original (in our case fractal) lattice and on the lattice that remains after a particular set of sites has been removed. This scheme, when repeated, then leads to the probability densities of waiting times for ever larger distances and longer times and allows the calculation of the scaling connection between distances and times.

The structures considered in this paper are described in detail in the preceding paper [1] (hereafter called I) and are special cases of the following model: we define a quasirandom fractal embedded in d-dimensional Euclidean space as one that consists of $d+1$ generators and a branching sequence in which one of the $d+1$ generators replaces each unit obtained at a previous step. The generators consist of branching structures containing $2,3,\ldots,d+1$ units. A generator with $k+1$ units replaces a previous unit with probability P_k, where the normalization condition $\sum_{k=1}^{d} P_k = 1$ must hold. For $d=2$ each generator has either two (collinear generator) or three units. The replacement of each unit by a given generator follows the construction rules introduced by Mandelbrot and Vicsek [5] in the context of a deterministic fractal growth model, the MV model, that they introduced in an effort to mimic some of the properties of DLA's. According to these construction rules (1) none of the branches may point in a direction below the horizontal and (2) no branches are allowed to overlap. The decimation procedure used to implement the renormalization scheme removes from explicit consideration the nearest neighbors that connect a site of origin to its next-nearest neighbors, including the branches that emerge from the nearest neighbors. This procedure is then repeated again and again, producing at each stage a structure that is statistically equivalent to the one that preceded it. An example of a quasirandom fractal structure in two dimensions is shown in Fig. 1.

The preceding paper deals with transport in the absence of external fields, that is, unbiased transport. In that case the hopping probability from an origin to any particular site is independent of the direction of that site relative to the backbone of the fractal structure and is the same for all "equidistant" sites, that is, for all nth-order neighbors of the origin. Furthermore, the mean first-passage time to a particular site is the same for all equidistant sites from the origin and is independent of direction. The mean first-passage time turns out to be insensitive to detailed features of the geometry of the structure and depends only on a weighted average of the

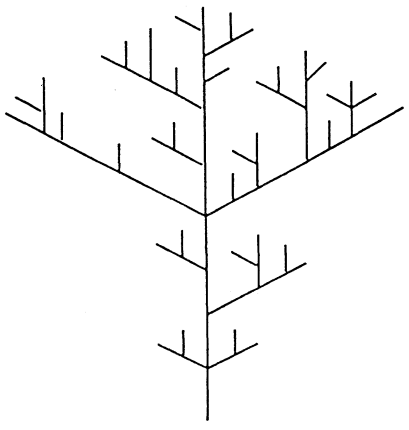

FIG. 1. Quasirandom fractal in two dimensions at the fourth stage of construction. Each generator has either two units (collinear generator) or three units.

branching structure.

The renormalization procedure was first developed by Machta [6] for a one-dimensional lattice and later by Van den Broeck [7] for a number of finitely ramified fractals. We have generalized their procedure to account for the presence of a field. In our earlier work we considered the first-passage-time distribution on a Sierpinski gasket [8] and found the scaling connections between time, distance, and field intensity. Herein we extend that analysis to biased walks on the structures introduced in I, namely the MV model as well as our quasirandom model. In particular, we consider the effect of an external field parallel to the backbone of the structure. The hopping probabilities and mean first-passage times to a given nth-order neighbor of a point of origin are no longer the same for all neighbors of a given order but rather depend on the location of that neighbor relative to the backbone.

We begin our analysis with a digression on notation in Sec. II; we expect that the necessary proliferation of symbols, subscripts, and superscripts is thereby made more manageable. In Sec. III we develop the renormalization scheme for a one-dimensional biased walk. Although such a walk is well understood and easily dealt with using other standard methods, the presentation helps to introduce our procedures in the simplest context. Section IV deals with biased walks on the MV model, while Sec. V deals with walks on the quasirandom model. We conclude with some observations in Sec. VI.

II. NOTATION

There is an inevitable proliferation of notation even in the unbiased walk considered in I to indicate all the possible physical quantities, points of origin, and nature of the branches involved in the random walk on the fractal structures that we consider. Thus we first introduced the hopping-time distribution $\psi_0(t)$ between a site of origin and any of its nearest neighbors and its Laplace transform $\tilde{\psi}_0(s)$. Next we generalized this definition to the hopping-time distribution $\psi_n(t)$ (and its associated Laplace transform) between the origin and any of its $(n+1)$st neighbors. For some of our fractals these distributions depend on the way in which the site of origin is connected to the rest of the structure, a dependence that we indicated via an additional superscript (i), as in $\psi_n^{(i)}$, which indicates the number of nearest neighbors of the origin. In some instances we needed to distinguish between different branching structures emerging from a *neighbor* of the site of origin, a dependence that we indicated via a second subscript in addition to the generation subscript n. From these hopping-time distributions we then went on to calculate hopping probabilities

$$\Psi_n^{(i)} \equiv \int_0^\infty dt \psi_n^{(i)}(t) = \tilde{\psi}_n(s=0) \tag{2.1}$$

and mean first-passage times

$$\langle t_n^{(i)} \rangle \equiv \int_0^\infty dt t \psi_n^{(i)}(t) = -\frac{d\tilde{\psi}_n^{(i)}(s)}{ds}\bigg|_{s=0} . \tag{2.2}$$

The situation in the presence of a field becomes considerably more complex for two reasons. First, it is no longer sufficient to indicate only the neighbor generation n from a given site: the properties of a walk to an $(n+1)$st neighbor now depend on the particular neighbor. Second, vertices of origin that were previously degenerate [in the sense that they fell under the same label (i)] may now differ from one another because, although their local configuration is the same, their orientation relative to the backbone of the structure differs. Our notation in this paper is therefore necessarily somewhat cumbersome and will be as indicated in Fig. 2, where we have drawn all the possible configurations of a site of origin and its nearest neighbors.

We distinguish six different types of vertices, indicated by greek letters. We also distinguish between different jump directions: all upward jumps parallel to the backbone are denoted by a p, those downward by a q, those upward but at an angle to the backbone by r, and those downward but at an angle by u. Each of these symbols then carries one of the six vertex-type subscripts indicating the type of vertex of origin and another subscript indicating the generation.

Thus, for example, the hopping-time distribution from a "dead-end" vertex to its nearest neighbor when this connection lies parallel to the fractal backbone will be denoted by $q_{\alpha,0}(t)$ and its Laplace transform by $\tilde{q}_{\alpha,0}(s)$. Further generations in the decimation process are indicated by increasing the second subscript. The hopping-time distribution from a dead-end vertex to its nearest neighbor when this connection lies at an angle to the

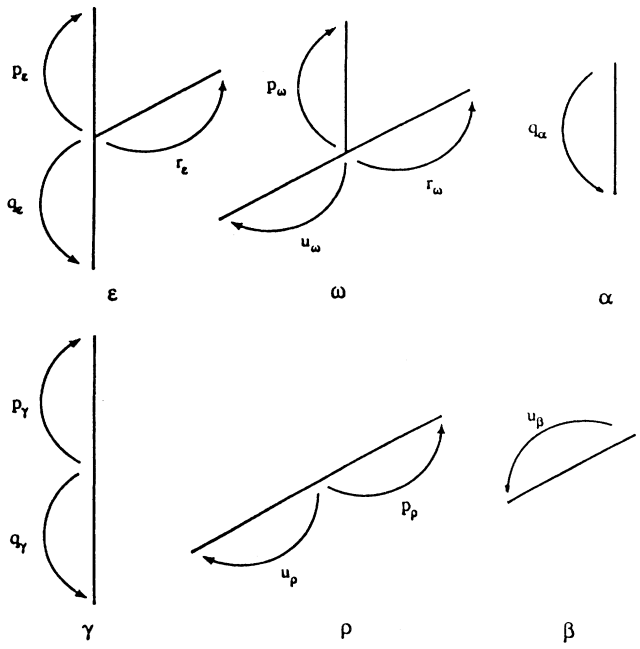

FIG. 2. All the possible configurations of a site of origin and its nearest neighbors, and associated notation, for the 12 distinct hopping-time distributions that arise in the quasirandom model. Note that only configurations α, β, ϵ, and ω and the 8 associated hopping time distributions arise in the MV model.

backbone of the structure will be denoted by $u_{\beta,0}(t)$. In the absence of an external field these two hopping-time distributions become equal to one another and are identified with the distribution $\psi_0^{(1)}(t)$ introduced earlier, that is, in the unbiased case

$$q_{\alpha,n}(t) = u_{\beta,n}(t) = \psi_n^{(1)}(t). \tag{2.3}$$

There are two types of vertices with two exits, those parallel to the backbone and those that lie at an angle to it. For the parallel case we denote the hopping-time distributions by $p_{\gamma,n}(t)$ and $q_{\gamma,n}(t)$ for upward and downward motion, respectively. If the branch lies at an angle to the backbone, the hopping-time distributions are denoted by $r_{\rho,n}(t)$ and $u_{\rho,n}(t)$. In the unbiased case these all become equal and reduce to

$$p_{\gamma,n}(t) = q_{\gamma,n}(t) = r_{\rho,n}(t) = u_{\rho,n}(t) = \frac{1}{2}\psi_n^{(2)}(t). \tag{2.4}$$

There are two distinct kinds of vertices with three emerging branches. We denote the respective hopping-time distributions by $p_{\epsilon,n}(t)$, $q_{\epsilon,n}(t)$, and $r_{\epsilon,n}(t)$ for one of these and $p_{\omega,n}(t)$, $u_{\omega,n}(t)$, and $r_{\omega,n}(t)$ for the other. In the unbiased case these also become equal and reduce to

$$p_{\epsilon,n}(t) = q_{\epsilon,n}(t) = r_{\epsilon,n}(t) = p_{\omega,n}(t) = u_{\omega,n}(t) = r_{\omega,n}(t) = \frac{1}{3}\psi_n^{(3)}(t). \tag{2.5}$$

The hopping probabilities associated with each of these hopping-time distributions, that is, the integrals of each of these over time, will again be denoted by the corresponding capital letters, e.g.,

$$P_{\epsilon,n} \equiv \int_0^\infty dt\, p_{\epsilon,n}(t) = \tilde{p}_{\epsilon,n}(s=0). \tag{2.6}$$

III. ANISOTROPIC ONE-DIMENSIONAL RANDOM WALK

In this section we detail the renormalization procedure for the familiar case of a biased walk in one dimension. This simple situation, which has been analyzed by Van den Broeck and Balakrishan [9] (and whose analysis we borrow), allows for the analytic solution of the problem to an extent that is not possible for the fractal structures, where our aims are necessarily somewhat more modest. We go further and relate the hopping-time distributions and associated hopping probabilities and first-passage times to the strength of the external field. These results offer insight into those found for more complex systems.

The one-dimensional system consists of a string of collinear vertices of the γ type in Fig. 2. The hopping-time distribution from each site to the site above is $p_{\gamma,0}(t)$ and to the site below is $q_{\gamma,0}(t)$. In the one-dimensional analysis we can dispense with the subscript γ since this is the only vertex we deal with. Furthermore, the one-dimensional chain is customarily drawn horizontally rather than vertically, so that $p_0(t)$ and $q_0(t)$ respectively label hopping-time distributions to the right and to the left (see Fig. 3). The hopping probability to a nearest neighbor on the right is P_0 and to the left is Q_0, respectively defined as

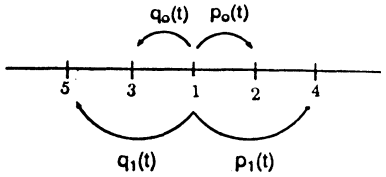

FIG. 3. One-dimensional biased continuous-time random walk which begins at site 1. Hopping-time distributions to nearest-neighbor sites 2 and 3 and to next-nearest-neighbor sites 4 and 5.

$$P_0 \equiv \int_0^\infty dt\, p_0(t), \qquad Q_0 \equiv \int_0^\infty dt\, q_0(t), \tag{3.1}$$

with $P_0 + Q_0 = 1$. In a symmetric (unbiased) random walk these would each be equal to 1/2.

A. Renormalization equations

We begin with the nearest-neighbor hopping-time distributions $p_0(t)$ and $q_0(t)$ and wish to calculate the distributions $p_1(t)$ and $q_1(t)$ to the next-nearest neighbors in terms of these. In order to do so, we now implement the decimation procedure described in I, that is, we remove the nearest neighbors 2 and 3 of the origin 1 in Fig. 3 from explicit consideration and sum over all the paths that lead to the next-nearest neighbor 4 before 5 to calculate $p_1(t)$, and those that lead to 5 before 4 to calculate $q_1(t)$. We must distinguish between arrival at 4 and at 5 since the hopping-time distributions to these sites are no longer equal to each other. Therefore, instead of obtaining a single renormalization equation connecting the nearest- and next-nearest-neighbor hopping-time distributions ψ_0 and ψ_1 we now obtain two coupled equations connecting p_1 and q_1 to p_0 and q_0. It is possible to obtain these equations by explicitly following all the possible paths as we did in I, and we do so in Appendix A. However, this process becomes especially cumbersome for the more complex structures considered subsequently, so instead we use a method that we introduced in [8] for the Sierpinski gasket to write the sums over all paths in compact matrix form.

For that purpose we define the matrix

$$\mathbf{A}_0(t) = \begin{pmatrix} 0 & p_0(t) & q_0(t) \\ q_0(t) & 0 & 0 \\ p_0(t) & 0 & 0 \end{pmatrix}. \tag{3.2}$$

The rows and columns of $\mathbf{A}$ correspond to the sites shown in Fig. 3, and the elements of the matrix are the hopping-time distributions between these sites on the original lattice. The diagonal elements are 0 because a walker does not hop from a site onto the same site. The (1,2) ele-

ment represents a hop from the origin to site 2, the (1,3) element a hop from the origin to site 3, etc. Since there are no direct hops between sites 2 and 3, the associated entries are zero.

Now suppose that we wish to calculate the hopping-time distribution $p_1(t)$ to the next-nearest neighbor 4. It is not difficult to convince oneself that this distribution is given in terms of the following convolution:

$$p_1(t) = \sum_{j=1}^{\infty} \langle 0| \int_0^t dt_{j-1} \cdots \int_0^{t_2} dt_1 \mathbf{A}_0(t_j - t_{j-1}) \cdots \mathbf{A}_0(t_2 - t_1)\mathbf{A}_0(t_1)|\nu_p(t - t_j)\rangle. \tag{3.3}$$

Here $\langle 0| \equiv (1 \quad 0 \quad 0)$ is a row vector that reflects the fact that the walker starts at site 1. The vector $|\nu_p(t)\rangle$ is a column vector constructed so as to identify the final site of interest and reflects the final step that the walker must take to arrive there. Thus, with site 4 as the goal, the final step must occur from site 2 to the right, and consequently $|\nu_p(t - t_j)\rangle$ has components $(0,\ p_0(t - t_j),\ 0)$ (in column vector form). If instead we wished to calculate the hopping-time distribution $q_1(t)$ to the next-nearest neighbor 5, then in (3.3) on the right-hand side $|\nu_p(t - t_j)\rangle$ would be replaced by $|\nu_q(t - t_j)\rangle$ with components $(0,\ 0,\ q_0(t - t_j))$ indicating the final step that the walker must take from site 3 to the left. Note that Eq. (3.3) in I is recovered from (3.3) above if one sets $p_0(t) = q_0(t) = \frac{1}{2}\psi_0(t)$. We subsume both of these cases into the single equation

$$x_1(t) = \sum_{j=1}^{\infty} \langle 0| \int_0^t dt_{j-1} \cdots \int_0^{t_2} dt_1 \mathbf{A}_0(t_j - t_{j-1}) \cdots \mathbf{A}_0(t_2 - t_1)\mathbf{A}_0(t_1)|\nu_x(t - t_j)\rangle, \tag{3.4}$$

where x stands for either p or q. The Laplace transform of (3.4), which replaces Eq. (3.4) of I and yields $\tilde{p}_1(s)$ and $\tilde{q}_1(s)$, then is

$$\tilde{x}_1(s) = \sum_{j=0}^{\infty} \langle 0|[\tilde{\mathbf{A}}_0(s)]^j|\tilde{\nu}_x(s)\rangle$$

$$= \langle 0|[1 - \tilde{\mathbf{A}}_0(s)]^{-1}|\tilde{\nu}_x(s)\rangle. \tag{3.5}$$

These are the renormalization equations after one decimation. These renormalization equations are valid at each stage of decimation, that is,

$$\tilde{x}_n(s) = \sum_{j=0}^{\infty} \langle 0|[\tilde{\mathbf{A}}_{n-1}(s)]^j|\tilde{\nu}_x(s)\rangle$$

$$= \langle 0|[1 - \tilde{\mathbf{A}}_{n-1}(s)]^{-1}|\tilde{\nu}_x(s)\rangle. \tag{3.6}$$

It is a simple matter to calculate the inverse in (3.6) with the matrix (3.2), and one easily finds upon performing the sum over j the explicit renormalization equations

$$\tilde{p}_n(s) = \frac{[\tilde{p}_{n-1}(s)]^2}{1 - 2\tilde{p}_{n-1}(s)\tilde{q}_{n-1}(s)}, \tag{3.7a}$$

$$\tilde{q}_n(s) = \frac{[\tilde{q}_{n-1}(s)]^2}{1 - 2\tilde{p}_{n-1}(s)\tilde{q}_{n-1}(s)}. \tag{3.7b}$$

Note that these renormalization equations are valid whether the walk is biased or unbiased. The information concerning the presence or absence of a bias only appears when one specifies the hopping-time distributions $p_0(t)$ and $q_0(t)$ on the original lattice, that is, the "initial conditions" for the recursion formulas. If these are equal (unbiased walk), then they remain equal for all subsequent generations, as can easily be seen from Eqs. (3.7). If they are not, then the evolution of the discrepancy for subsequent generations must be found from Eqs. (3.7). In any case, the renormalization equations (3.7a) and (3.7b) can be solved explicitly for all s, something that is not possible for our more complex structures. Here we take advantage of the fact that we can exhibit the full solution in this case.

B. Solution of renormalization equations

The full solution of the renormalization equations is accomplished by noting that Eqs. (3.7) imply that [9]

$$\frac{\tilde{p}_n(s)}{\tilde{q}_n(s)} = \left[\frac{\tilde{p}_{n-1}(s)}{\tilde{q}_{n-1}(s)}\right]^2 = \left[\frac{\tilde{p}_0(s)}{\tilde{q}_0(s)}\right]^{2^n} \tag{3.8}$$

and that

$$\frac{1}{\sqrt{4\tilde{p}_n(s)\tilde{q}_n(s)}} = T_2\left(\frac{1}{\sqrt{4\tilde{p}_{n-1}(s)\tilde{q}_{n-1}(s)}}\right)$$

$$= \cosh\left[2^n \cosh^{-1}\left(\frac{1}{\sqrt{4\tilde{p}_0(s)\tilde{q}_0(s)}}\right)\right], \tag{3.9}$$

where T_2 is the Chebyshev polynomial of order 2 [10]. The solution for the renormalization equation is obtained by combining (3.8) and (3.9):

$$\tilde{p}_n(s) = \left[\sqrt{\tilde{p}_0(s)/\tilde{q}_0(s)}\right]^{2^n} \times \frac{1}{2\cosh\left[2^n \cosh^{-1}\left(\frac{1}{\sqrt{4\tilde{p}_0(s)\tilde{q}_0(s)}}\right)\right]}, \tag{3.10a}$$

$$\tilde{q}_n(s) = \left[\sqrt{\tilde{q}_0(s)/\tilde{p}_0(s)}\right]^{2^n} \times \frac{1}{2\cosh\left[2^n \cosh^{-1}\left(\frac{1}{\sqrt{4\tilde{p}_0(s)\tilde{q}_0(s)}}\right)\right]}. \tag{3.10b}$$

Consider now the particular and familiar case of a Markov process, that is, one in which the hopping-time distributions in the original lattice are exponential. We further assume that the jump rate parameter λ for jumps to the right and the left are the same, so that the asymmetry in jumps to right and left occurs only because of the difference in the total hopping probabilities in these directions. Thus

$$p_0(t) = P_0 \lambda e^{-\lambda t}, \qquad q_0(t) = Q_0 \lambda e^{-\lambda t}, \tag{3.11}$$

and consequently

$$\tilde{p}_0(s) = P_0 \frac{\lambda}{\lambda + s}, \qquad \tilde{q}_0(s) = Q_0 \frac{\lambda}{\lambda + s}. \tag{3.12}$$

With these initial conditions the full solution of the renormalization equations is

$$\tilde{p}_n(s) = \left(\sqrt{P_0/Q_0}\right)^{2^n} \frac{1}{2\cosh\left[2^n \cosh^{-1}\left(\frac{\lambda + s}{2\lambda\sqrt{P_0 Q_0}}\right)\right]}, \tag{3.13a}$$

$$\tilde{q}_n(s) = \left(\sqrt{Q_0/P_0}\right)^{2^n} \frac{1}{2\cosh\left[2^n \cosh^{-1}\left(\frac{\lambda + s}{2\lambda\sqrt{Q_0 P_0}}\right)\right]}. \tag{3.13b}$$

In particular, we can use this solution to calculate the asymptotic hopping probabilities and mean first-passage times.

The asymptotic hopping probabilities are obtained from Eqs. (3.13) in the limit $n \to \infty$. One readily finds the following result:

$$P \equiv \lim_{n\to\infty} P_n = \begin{cases} 0, & P_0 < 1/2 \\ 1/2, & P_0 = 1/2 \\ 1, & P_0 > 1/2. \end{cases} \tag{3.14}$$

Thus, if the probability of going to the right on the original lattice is smaller than that of going to the left, then asymptotically the walker will certainly walk to the left; conversely, if the initial probability of going to the right is greater, then asymptotically the walker will certainly walk to the right. If the left and right probabilities are initially equal, they will remain so for all times.

The first-passage time for arrival at either of the nth neighbors of the origin can also be evaluated from the derivatives of (3.13a) and (3.13b) with respect to s at $s = 0$ [cf. Eq. (2.2)]. Conversely, we could take these derivatives in Eqs. (3.7a) and (3.7b) to find $\langle t_n \rangle$ in terms of $\langle t_{n-1} \rangle$ and then we could directly solve this recursion relation. This was the procedure followed in I and is the appropriate method when we cannot solve the full renormalization equations. We defer the calculation of the first-passage time to Sec. III C, where we first relate the parameters P_0 and Q_0 to ones that are physically more transparent.

C. Parameters of the model

It is physically instructive to relate the initial condition (3.11) of the renormalization flow to the external field causing the anisotropy and to the elementary hopping rates on the original lattice.

The rate of escape from one site to any nearest-neighboring site in the absence of a field is denoted by Γ_0. The presence of a constant external force $\mathbf{F}$ of magnitude F introduces a bias so that jumps against the external field occur at a lower rate than those in the direction of the field. The new rate of escape is [11,12]

$$\Gamma_{ij} = \Gamma_0 \exp\left(\frac{1}{2}\beta \mathbf{F} \cdot \mathbf{r}_{ij}\right), \tag{3.15}$$

where $\mathbf{r}_{ij}$ is the vector that joins the nearest-neighbor sites i and j, $\beta = 1/kT$, and T denotes temperature.

In our one-dimensional system we take the field to point toward the left and denote the nearest-neighbor distance by Δx so that Eq. (3.15) can be rewritten as

$$\Gamma_{i,i\pm1} = \Gamma_0 \exp\left(\pm\frac{1}{2}\beta F \Delta x\right). \tag{3.16}$$

In the case of Markovian initial waiting-time distributions (3.11) we identify the total jump rate with the quantity λ introduced earlier, that is,

$$\lambda = \Gamma_0 e^{(1/2)\beta F \Delta x} + \Gamma_0 e^{-(1/2)\beta F \Delta x} = 2\Gamma_0 \cosh\left(\frac{1}{2}\beta F \Delta x\right), \tag{3.17}$$

and the hopping probabilities appearing in the coefficients with the ratios $\Gamma_{i,i\pm1}/\lambda$:

$$P_0 = \frac{e^{-\frac{1}{2}\beta F \Delta x}}{e^{\frac{1}{2}\beta F \Delta x} + e^{-\frac{1}{2}\beta F \Delta x}} = \frac{1}{e^{\beta F \Delta x} + 1}, \tag{3.18a}$$

$$Q_0 = \frac{e^{\frac{1}{2}\beta F \Delta x}}{e^{\frac{1}{2}\beta F \Delta x} + e^{-\frac{1}{2}\beta F \Delta x}} = \frac{e^{\beta F \Delta x}}{e^{\beta F \Delta x} + 1}. \tag{3.18b}$$

Consequently we have for the Laplace transforms (3.12)

$$\tilde{p}_0(s) = \Gamma_0 \frac{\exp\left(-\frac{1}{2}\beta F \Delta x\right)}{s + 2\Gamma_0 \cosh\left(\frac{1}{2}\beta F \Delta x\right)}, \tag{3.19a}$$

$$\tilde{q}_0(s) = \Gamma_0 \frac{\exp\left(\frac{1}{2}\beta F \Delta x\right)}{s + 2\Gamma_0 \cosh\left(\frac{1}{2}\beta F \Delta x\right)}. \tag{3.19b}$$

D. Hopping probabilities and mean first-passage times

We can now use the identifications (3.17) and (3.19) to write the full solution (3.13) in terms of the temperature

and the external field,

$$\tilde{p}_n(s) = \frac{\exp\left(-\frac{1}{2}\beta F x_n\right)}{2\cosh\left[\sqrt{(\frac{1}{2}\beta F x_n)^2 + 4^n s/\Gamma_0}\right]}, \tag{3.20a}$$

$$\tilde{q}_n(s) = \frac{\exp\left(\frac{1}{2}\beta F x_n\right)}{2\cosh\left[\sqrt{(\frac{1}{2}\beta F x_n)^2 + 4^n s/\Gamma_0}\right]}. \tag{3.20b}$$

In this relation we have set $x_n \equiv 2^n \Delta x$ = the distance covered by one step in the nth generation, which is twice the distance covered in the previous generation. Note that these definitions reflect the distance and time scaling of the isotropic problem, where twice the distance takes four times longer to cover (ordinary diffusion).

Let us now consider the hopping probabilities and first-passage times implied by these results. The former are obtained by setting $s = 0$ in (3.20):

$$P_n = \frac{1}{e^{\beta F x_n} + 1}, \qquad Q_n = \frac{e^{\beta F x_n}}{e^{\beta F x_n} + 1}. \tag{3.21}$$

As $n \to \infty$, since x_n grows without bound, this result reproduces (3.14) for $P_0 \leq 1/2$. However, more information can be extracted from these results if instead we rescale the external field in such a way that Fx_n remains finite even as n grows without bound, that is, we allow the field over a distance Δx to become smaller and smaller (as 2^{-n}) as the distances that we are interested in grow (double at each generation) relative to the nearest-neighbor distance on the lattice in such a way that the potential Fx_n over the distance of interest remains finite. Thus we rescale the force F as $F \to F_n = F2^{-n}$ so that at each step (and, in particular, as $n \to \infty$) we can set $F_n x_n = F\Delta x \equiv Fx$ = finite independently of n where x is the (usually macroscopic) distance of interest and F is the force acting over that distance. We then rewrite $P_n \equiv P(x,F)$ and $Q_n \equiv Q(x,F)$ of (3.21) as

$$P(x,F) = \frac{1}{e^{\beta F x} + 1}, \quad Q(x,F) = \frac{e^{\beta F x}}{e^{\beta F x} + 1}. \tag{3.22}$$

These relations then give the dependence of the hopping probabilities on the hopping distance and the external force via the product Fx. If Fx goes strictly to infinity, we recover (3.14).

Next we consider the mean first-passage time to an nth neighbor (or to a distance x) to the right or left of the origin:

$$\langle t_n \rangle = -\left.\frac{d\tilde{p}_n(s)}{ds}\right|_{s=0} - \left.\frac{d\tilde{q}_n(s)}{ds}\right|_{s=0}. \tag{3.23}$$

The time $\langle t_n \rangle$ is of course determined primarily by the time it takes to reach the neighbor to the left since the field biases the walk in that direction. The mean first-passage time can be calculated directly from (3.20a) and (3.20b), or we can go back to the renormalization equations (3.7a) and (3.7b) and use those to establish a recursion relation that can then be solved. The former method is more straightforward—it leads to the result in one step. However, since we usually cannot solve the renormalization equations analytically, it is instructive to illustrate the second method, which is the one that has to be used in more complicated cases.

We denote the appropriate derivatives of the Laplace transforms of the hopping probabilities evaluated at $s = 0$ as follows:

$$\tilde{p}'_n \equiv \left.\frac{d\tilde{p}_n(s)}{ds}\right|_{s=0}, \qquad \tilde{q}'_n \equiv \left.\frac{d\tilde{q}_n(s)}{ds}\right|_{s=0}. \tag{3.24}$$

Taking derivatives of the renormalization equations (3.7a) and (3.7b) we can then construct the relations

$$\begin{pmatrix} \tilde{p}'_n \\ \tilde{q}'_n \end{pmatrix} = \mathbf{J}_n(0) \begin{pmatrix} \tilde{p}'_{n-1} \\ \tilde{q}'_{n-1} \end{pmatrix}. \tag{3.25}$$

The 2×2 Jacobian coefficient matrix $\mathbf{J}_n(0)$ is given by

$$\mathbf{J}_n(0) = \begin{pmatrix} \dfrac{2P_n^2 Q_n}{(1-2P_nQ_n)^2} + \dfrac{2P_n}{1-2P_nQ_n} & \dfrac{2P_n^3}{(1-2P_nQ_n)^2} \\ \dfrac{2Q_n^3}{(1-2P_nQ_n)^2} & \dfrac{2Q_n^2 P_n}{(1-2P_nQ_n)^2} + \dfrac{2Q_n}{1-2P_nQ_n} \end{pmatrix}, \tag{3.26}$$

where the P_n and Q_n are given in Eq. (3.21). This recursion relation can be solved as a 2×2 matrix recursion relation, but it turns out that the sum of the elements of column 1 is equal to the sum of the elements of column 2 when the substitution $p = 1 - q$ is made. This allows us to construct a direct recursion relation for the mean first-passage time:

$$\begin{aligned} \langle t_n \rangle &= -\tilde{p}'_n - \tilde{q}'_n \\ &= -J_{11}\tilde{p}'_{n-1} - J_{12}\tilde{q}'_{n-1} - J_{21}\tilde{p}'_{n-1} - J_{22}\tilde{q}'_{n-1} \\ &= (J_{11} + J_{21})\langle t_{n-1} \rangle. \end{aligned} \tag{3.27}$$

The solution of the recursion relation (3.27) is [as can also readily be obtained by direct derivates of (3.20a) and (3.20b)]

$$\langle t_n \rangle = \frac{4^n}{2\Gamma_0} \frac{\tanh\left(\frac{1}{2}\beta F_n x_n\right)}{\frac{1}{2}\beta F_n x_n}. \tag{3.28}$$

Again, in order for this result to be sensible as $n \to \infty$ we rescale the external force as we did earlier. Furthermore, we introduce the "effective" hopping rate $\Gamma_n = 1/4^n t_0$ (which is independent of the external force) and introduce a scaling of this rate which ensures the correct diffusive limit when the external field is vanishingly small:

$$t_0\Gamma_n = \left(\frac{\Delta x}{x_n}\right)^2 = \left(\frac{\Delta x}{2^n \Delta x}\right)^2. \tag{3.29}$$

(In other words, we are setting $4^n = 2^{2n}$.) As a function of the scaled continuous variables we then rewrite (3.28) as

$$\langle t(x,F)\rangle = \frac{x^2}{2\Gamma_0 \Delta x^2} \frac{\tanh\left(\frac{1}{2}\beta F x\right)}{\frac{1}{2}\beta F x}$$

$$= \frac{x}{D\beta F} \tanh\left(\frac{1}{2}\beta F x\right), \tag{3.30}$$

where we have set $2\Gamma_0 \Delta x^2 \equiv D$, an effective diffusion coefficient. This result then characterizes the way in which the mean first-passage time varies with the distance and the external force (see Fig. 4).

It is instructive to define a field-dependent random walk dimension d_w [13,14] such that Eq. (3.30) can be written in the usual way as

$$\langle t(x,F)\rangle = \frac{x}{D\beta F} \tanh\left(\frac{1}{2}\beta F x\right) = D x^{d_w}. \tag{3.31}$$

Clearly,

$$d_w = \frac{\ln\left(\frac{2(1+e^{\beta F x})^2}{(1+e^{2\beta F x})}\right)}{\ln 2}. \tag{3.32}$$

The associated spectral dimension $d_s = 2d_f/d_w$ with $d_f = 1$ (see I) is

$$d_s = \frac{2\ln 2}{\ln\left(\frac{2(1+e^{\beta F x})^2}{(1+e^{2\beta F x})}\right)} \tag{3.33}$$

(see Fig. 5). As a check of these scaling choices, we note

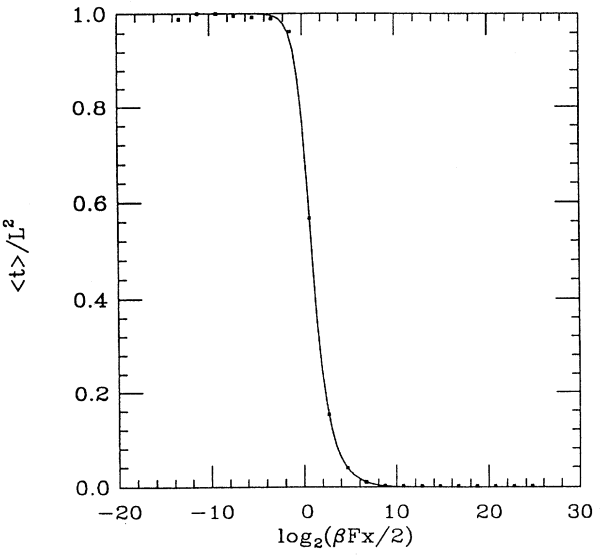

FIG. 4. Mean first-passage time as a function of distance and external field for a one-dimensional biased nearest-neighbor random walk. Solid curve, analytic results; solid circles, direct simulations.

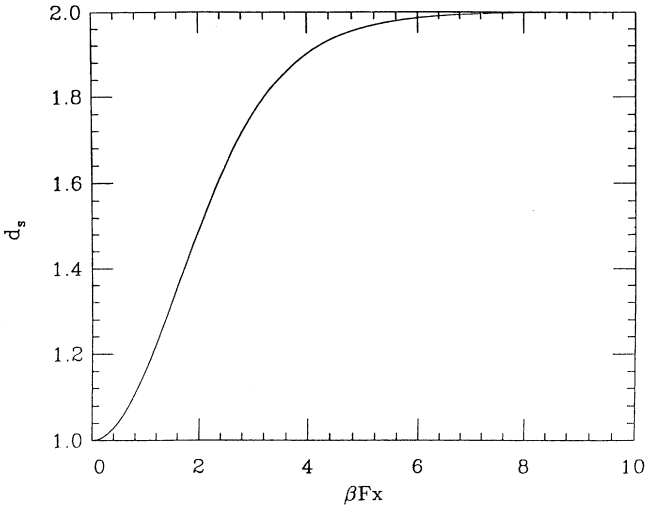

FIG. 5. Effective spectral dimension of the one-dimensional biased random walk as a function of distance and field strength.

that when Fx is small, Eq. (3.30) reduces to

$$\langle t(x)\rangle \sim x^2/2D, \tag{3.34}$$

independent of F, which is indeed the usual diffusive motion result relating the square of the displacement to the time, as appropriate for an unbiased walk; at these small distances and/or weak forces the walker does not yet have an opportunity to "feel" the effects of the force. The spectral dimension in this limit approaches unity, $d_s \to 1$, as appropriate for Brownian motion in one dimension (compact random walk). When Fx is large the mean first-passage time (3.30) becomes

$$\langle t(x,F)\rangle \sim \frac{x}{D\beta F} = \frac{xkT}{DF}. \tag{3.35}$$

The mean first-passage time to cover a given distance is now proportional to the distance (characteristic of biased motion) and inversely proportional to the external force. The spectral dimension $d_s \to 2$, as appropriate for a random walk in which each step on the average takes the walker to a new site.

IV. BIASED WALK ON THE TWO-DIMENSIONAL MV MODEL

Consider the effects of a field parallel to the backbone of an MV structure. When such a field is turned on, instead of the single hopping probability density $\psi_n(t)$ that occurred in I we now have to consider eight different ones: one in Fig. 2 associated with the vertex α, one with β, three with ϵ, and three with ω.

In I we distinguished between a "dead-end" vertex and a "normal" vertex. Now we must make finer distinctions because previously degenerate situations are differentiated by the field. In particular, we must distinguish

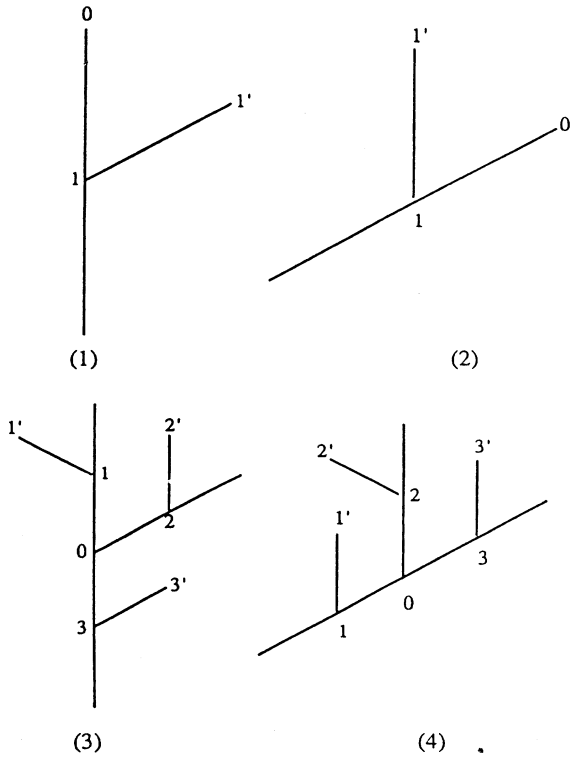

FIG. 6. Four different vertices that must be considered separately in the MV model.

between two dead-end vertices and between two normal vertices, shown in Fig. 6.

A. Renormalization equations

The decimation procedure that leads to the renormalization equations proceeds as in the one-dimensional case, but now the matrix $\mathbf{A}_0(t)$ and the other associated quantities are considerably more complex than in Sec. III. In particular, in place of Eq. (3.5) we now have

$$\tilde{x}_1^{(k)}(s) = \langle 0|[1 - \tilde{\mathbf{A}}_0^{(k)}(s)]^{-1}|\tilde{\nu}_{x^{(k)}}(s)|\rangle, \tag{4.1}$$

where $x^{(k)}$ stands for each one of the eight distinct hopping time distributions that arise in this model (cf. Fig. 2) and the superscript (k) with $k = 1, 2, 3, 4$ labels each of the four types of vertices. The elements of the matrices $\mathbf{A}_0^{(k)}(t)$ are the probability densities for hops among the origin of vertex k and the sites to be removed at the next decimation. We exhibit these four matrices explicitly in Appendix B. The vector $\langle 0|$ stands for (1 0 0) when $k = 1$ and $k = 2$ and for (1 0 0 0 0 0 0 0) when $k = 3$ and $k = 4$. The column vectors $|\nu_{x^{(k)}}(t)\rangle$ again reflect the final step that the walker must take to arrive at the site of interest and are also listed in Appendix B.

As before, the renormalization equations repeat exactly after each stage of decimation, so that (4.1) connects the nth generation to the $(n-1)$st for all n. Inverting the matrices $\tilde{\mathbf{A}}_{n-1}(s)$ explicitly then leads to the following set of coupled renormalization equations for the Laplace transforms of the hopping probability densities (we omit the arguments s):

$$\begin{aligned}
\tilde{p}_{\epsilon,n+1} &= \frac{(1-\tilde{p}_{\omega,n}\,\tilde{q}_{\alpha,n})\,\tilde{p}_{\epsilon,n}^2}{\tilde{D}_{1,n}},\\
\tilde{q}_{\epsilon,n+1} &= \frac{(1-\tilde{p}_{\omega,n}\,\tilde{q}_{\alpha,n})\,\tilde{q}_{\epsilon,n}^2}{\tilde{D}_{1,n}},\\
\tilde{r}_{\epsilon,n+1} &= \frac{(1-\tilde{u}_{\beta,n}\,\tilde{r}_{\epsilon,n})\,\tilde{r}_{\epsilon,n}\,\tilde{r}_{\omega,n}}{\tilde{D}_{1,n}},\\
\tilde{p}_{\omega,n+1} &= \frac{(1-\tilde{p}_{\omega,n}\,\tilde{q}_{\alpha,n})\,\tilde{p}_{\omega,n}\,\tilde{p}_{\epsilon,n}}{\tilde{D}_{2,n}},\\
\tilde{u}_{\omega,n+1} &= \frac{(1-\tilde{u}_{\beta,n}\,\tilde{r}_{\epsilon,n})\,\tilde{q}_{\omega,n}^2}{\tilde{D}_{2,n}},\\
\tilde{r}_{\omega,n+1} &= \frac{(1-\tilde{u}_{\beta,n}\,\tilde{r}_{\epsilon,n})\,\tilde{r}_{\omega,n}^2}{\tilde{D}_{2,n}},\\
\tilde{u}_{\beta,n+1} &= \frac{\tilde{u}_{\omega,n}\,\tilde{u}_{\beta,n}}{\tilde{D}_{3,n}},\\
\tilde{q}_{\alpha,n+1} &= \frac{\tilde{q}_{\epsilon,n}\,\tilde{q}_{\alpha,n}}{\tilde{D}_{4,n}},
\end{aligned} \tag{4.2}$$

where

$$\begin{aligned}
\tilde{D}_{1,n}(s) &= \tilde{u}_{\omega,n}\tilde{u}_{\beta,n}\tilde{r}_{\epsilon,n}^2 + (\tilde{p}_{\omega,n}\tilde{u}_{\beta,n}\tilde{q}_{\alpha,n}\\
&\qquad - \tilde{u}_{\beta,n} - \tilde{u}_{\omega,n})\tilde{r}_{\epsilon,n}\\
&\quad +(2\tilde{p}_{\epsilon,n}\tilde{q}_{\epsilon,n} - 1)\tilde{p}_{\omega,n}\tilde{q}_{\alpha,n} - 2\tilde{p}_{\epsilon,n}\tilde{q}_{\epsilon,n} + 1,\\
\tilde{D}_{2,n}(s) &= (2\tilde{u}_{\beta,n}\tilde{r}_{\epsilon,n} - 2)\tilde{u}_{\omega,n}\tilde{r}_{\omega,n}\\
&\quad +(\tilde{p}_{\omega,n}\tilde{q}_{\alpha,n} - 1)\tilde{u}_{\beta,n}\tilde{r}_{\epsilon,n}\\
&\quad +(\tilde{p}_{\omega,n}^2\tilde{q}_{\epsilon,n} - \tilde{p}_{\omega,n})\tilde{q}_{\alpha,n} - \tilde{p}_{\omega,n}\tilde{q}_{\epsilon,n} + 1,\\
\tilde{D}_{3,n}(s) &= 1 - \tilde{u}_{\beta,n}\tilde{r}_{\omega,n} - \tilde{p}_{\omega,n}\tilde{q}_{\alpha,n},\\
\tilde{D}_{4,n}(s) &= 1 - \tilde{u}_{\beta,n}\tilde{r}_{\epsilon,n} - \tilde{p}_{\epsilon,n}\tilde{q}_{\alpha,n}.
\end{aligned} \tag{4.3}$$

It is difficult to find the analytic solution for these renormalization equations. Instead, we concentrate directly on the prediction provided by these equations for the hopping probabilities and mean first-passage times. As in the one-dimensional walk, it is useful first to choose initial conditions for the flow and then to relate the parameters in these initial conditions to the external field and the elementary hopping rate on the original structure.

B. Parameters of the model

As in Sec. III, we begin by introducing a rate of escape Γ_0 from one site to another on the original undecimated structure. In the presence of a field (which we take to point upward along the backbone of the structure), the escape rates in all directions are no longer isotropic. Instead, we must now differentiate among the following four escape rates (the arrow subscripts indicate the direction of the jump):

$$\Gamma_{\uparrow} = \Gamma_0 \exp\left(\frac{1}{2}\beta F \Delta x\right),$$
$$\Gamma_{\downarrow} = \Gamma_0 \exp\left(-\frac{1}{2}\beta F \Delta x\right),$$
$$\Gamma_{\nearrow} = \Gamma_0 \exp\left(\frac{1}{2}\mu\beta F \Delta x\right),$$
$$\Gamma_{\swarrow} = \Gamma_0 \exp\left(-\frac{1}{2}\mu\beta F \Delta x\right). \tag{4.4}$$

Here $\mu = \cos\theta$ and θ is the angle between the angled branches and the backbone of the structure. As before, we assume that the hopping distributions on the original structure are exponential [cf. Eq. (3.11)] and identify a total jump rate out of each vertex. Instead of a single λ we must now identify four because we have four different vertices:

$$\lambda_\alpha = \Gamma_{\downarrow},$$
$$\lambda_\beta = \Gamma_{\swarrow},$$
$$\lambda_\epsilon = \Gamma_{\uparrow} + \Gamma_{\downarrow} + \Gamma_{\nearrow},$$
$$\lambda_\omega = \Gamma_{\uparrow} + \Gamma_{\swarrow} + \Gamma_{\nearrow}. \tag{4.5}$$

The anisotropies in each vertex are again associated with the differences in the total hopping probabilities in the various directions. We thus have for the eight different initial hopping probabilities the following ratios:

$$Q_{\alpha,0} = \frac{\Gamma_{\downarrow}}{\lambda_\alpha} = 1, \tag{4.6a}$$
$$U_{\beta,0} = \frac{\Gamma_{\swarrow}}{\lambda_\beta} = 1, \tag{4.6b}$$
$$P_{\epsilon,0} = \frac{\Gamma_{\uparrow}}{\lambda_\epsilon}, \tag{4.6c}$$
$$Q_{\epsilon,0} = \frac{\Gamma_{\downarrow}}{\lambda_\epsilon}, \tag{4.6d}$$
$$R_{\epsilon,0} = \frac{\Gamma_{\nearrow}}{\lambda_\epsilon}, \tag{4.6e}$$
$$P_{\omega,0} = \frac{\Gamma_{\uparrow}}{\lambda_\omega}, \tag{4.6f}$$
$$U_{\omega,0} = \frac{\Gamma_{\swarrow}}{\lambda_\omega}, \tag{4.6g}$$
$$R_{\omega,0} = \frac{\Gamma_{\nearrow}}{\lambda_\omega}. \tag{4.6h}$$

C. Analytic solution for hopping probabilities

Upon setting $s = 0$, the renormalization equations (4.2) become equations directly for the hopping probabilities that can be solved subject to the initial conditions (4.6a)–(4.6h). There is clearly nothing further to do concerning the vertices α and β: since they are dead-end vertices and there is only one way to leave them, it is easy to see that indeed $Q_{\alpha,n} = U_{\beta,n} = 1$ for all n. The six remaining hopping probabilities can be determined from three recursion equations together with the obvious probability conservation conditions

$$P_{\epsilon,n} + Q_{\epsilon,n} + R_{\epsilon,n} = 1, \tag{4.7a}$$
$$P_{\omega,n} + U_{\omega,n} + R_{\omega,n} = 1. \tag{4.7b}$$

The solutions of the remaining recursion equations for the hopping probabilities then become transparent if we consider instead the ratios

$$K_{\epsilon,n} = \frac{P_{\epsilon,n}}{Q_{\epsilon,n}}, \tag{4.8}$$

$$K_{\omega,n} = \frac{R_{\omega,n}}{U_{\omega,n}}, \tag{4.9}$$

$$C_n = \frac{P_{\epsilon,n}}{R_{\epsilon,n}} = \frac{P_{\omega,n}}{R_{\omega,n}}. \tag{4.10}$$

These ratios satisfy the equations

$$K_{\epsilon,n} = K_{\epsilon,n-1}^2, \tag{4.11}$$

$$K_{\omega,n} = K_{\omega,n-1}^2, \tag{4.12}$$

$$C_n = \frac{K_{\epsilon,n-1}\,(1 + K_{\omega,n-1})\,C_{n-1}}{K_{\omega,n-1}\,(1 + K_{\epsilon,n-1})}. \tag{4.13}$$

The solution of these three equations is completely straightforward since each generation is connected to the previous one through simple power relations. Thus first solving for the K's and then with these solutions finding C one obtains expressions with exponentials analogous to (3.21). As in that case, sensible solutions as $n \to \infty$ are obtained if ever increasing distances and ever stronger fields are scaled by factors of 2^n. The procedure is identical to that carried out in Sec. III, and finally we obtain for the hopping probabilities associated with vertices ϵ and ω in terms of the distance x and the force strength F:

$$P_\epsilon(x,F) = \frac{1 - e^{-\mu\beta F x}}{N_\epsilon(x,F)}, \tag{4.14a}$$

$$Q_\epsilon(x,F) = \frac{e^{-\beta F x}\left(1 - e^{-\mu\beta F x}\right)}{N_\epsilon(x,F)}, \tag{4.14b}$$

$$R_\epsilon(x,F) = \frac{\mu\left(1 - e^{-\beta F x}\right)}{N_\epsilon(x,F)}, \tag{4.14c}$$

$$P_\omega(x,F) = \frac{1 - e^{-\mu\beta F x}}{N_\omega(x,F)}, \tag{4.14d}$$

$$U_\omega(x,F) = \frac{\mu e^{-\beta F x}\left(1 - e^{-\mu\beta F x}\right)}{N_\omega(x,F)}, \tag{4.14e}$$

$$R_\omega(x,F) = \frac{\mu\left(1 - e^{-\beta F x}\right)}{N_\omega(x,F)}, \tag{4.14f}$$

where we recall that μ is the cosine of the angle between the angled branches and the backbone, and where

$$N_\epsilon(x,F) = \left(1 - e^{-\mu\beta F x}\right)\left(1 + e^{-\beta F x}\right) + \mu\left(1 - e^{-\beta F x}\right), \tag{4.15a}$$

$$N_\omega(x,F) = \mu\left(1 + e^{-\mu\beta F x}\right)\left(1 - e^{-\beta F x}\right) + \left(1 - e^{-\mu\beta F x}\right). \tag{4.15b}$$

The asymptotic behavior of the hopping probabilities [as $Fx \to \infty$, that is, in the strict limit also considered in (3.14)] can be obtained directly from (4.14a)–(4.14f):

$$P_\epsilon \to \frac{1}{1+\mu}, \tag{4.16a}$$

$$Q_\epsilon \to 0, \tag{4.16b}$$

$$R_\epsilon \to \frac{\mu}{1+\mu}, \tag{4.16c}$$

$$P_\omega \to \frac{1}{1+\mu}, \tag{4.16d}$$

$$U_\omega \to 0, \tag{4.16e}$$

$$R_\omega \to \frac{\mu}{1+\mu}. \tag{4.16f}$$

These results can be deduced from a deterministic analysis and reflect the behavior induced by a field that totally overshadows the random effects of stochastic motion.

The hopping probabilities (4.14a)–(4.14f) are plotted in Fig. 7 (for vertex ϵ) and in Fig. 8 (for vertex ω) as a function of Fx for two values of the angle of the branches relative to the backbone. The figures thus reflect the dependence of the hopping probabilities on the external force and also on the hopping distance. For each angle

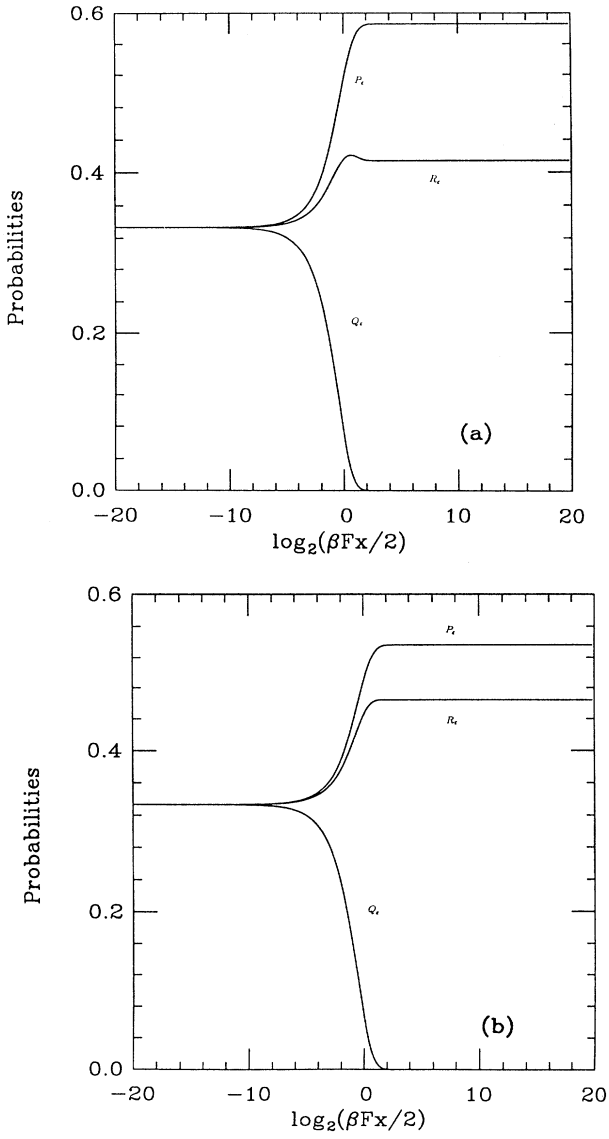

FIG. 7. Hopping probabilities for vertex ϵ in the two-dimensional MV model as a function of external field strength F and distance x for two values of the angle of the branches relative to the backbone. (a) $\theta = \pi/4$; (b) $\theta = \pi/5$.

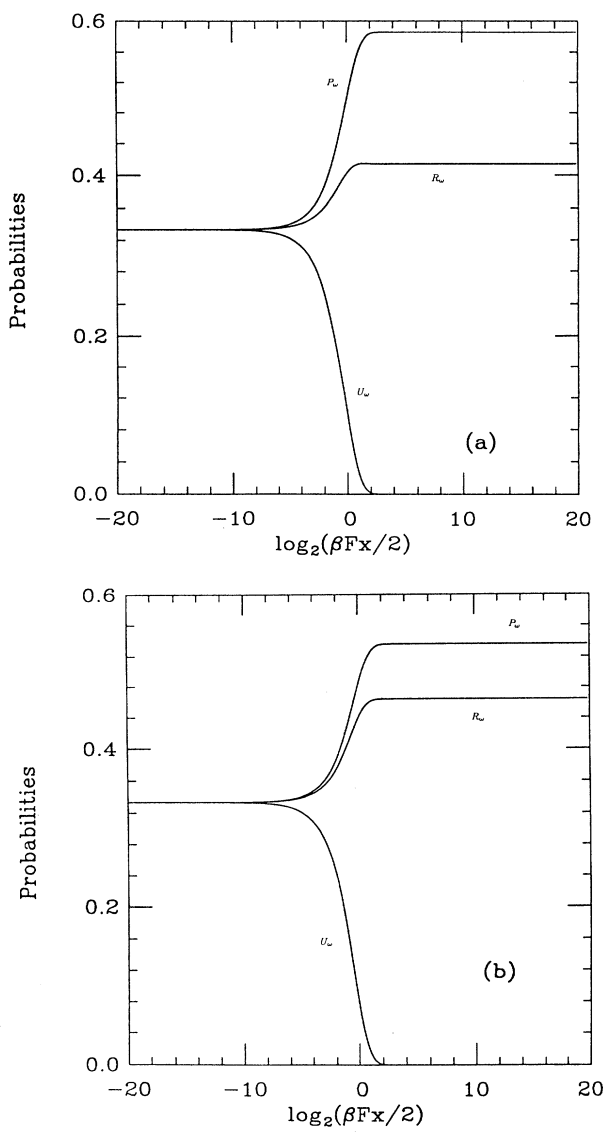

FIG. 8. Hopping probabilities for vertex ω in the two-dimensional MV model as a function of external field strength F and distance x for two values of the angle of the branches relative to the backbone. (a) $\theta = \pi/4$; (b) $\theta = \pi/6$.

the probabilities of moving up the structure in the direction of the field (the P's) increase monotonically and achieve the asymptotic value given in (4.16a) and (4.16d), which increases with decreasing μ. The latter trend reflects the fact that the angled branches "compete" with the vertical branches more effectively as the angle decreases. The probabilities Q and U of moving in a direction that has any component opposing the field decreases monotonically to zero. The most interesting field and distance dependence is observed in the probabilities R of diffusing in a direction that has an upward component but is not parallel to the field. With increasing Fx, these probabilities reflect the competition between the P and R pathways. As the field increases, more particles move in the P and R directions at the expense of the downward Q and U directions. The probability of moving along the R directions is of course always smaller than that of moving upward parallel to the field. For large values of the angle (which, however, is constrained to be smaller than $\pi/2$), the probabilities R first grow, achieve a maximum, and then decrease (in favor of the P's). If the angle is small, then the R's simply grow monotonically. In any case, the R's eventually achieve the asymptotic value $\mu/(\mu+1)$ of Eqs. (4.16c) and (4.16f). This asymptotic value increases with increasing μ, that is, the R direction competes more successfully with the upward motion as the branch angle decreases. We note that the nonmonotonic behavior of the R's is not a consequence of the fractal nature of the structure but rather of the angles of the pathways relative to the external field. An essentially one-dimensional structure with single branches pointing off the spine at regular intervals would exhibit the same sort of behavior.

D. Mean first-passage times for weak and strong fields

The mean first-passage times to reach a site a distance x away from a vertex of origin on a MV structure depend on the vertex of origin and must therefore carry appropriate labels to differentiate among four different mean first-passage times. Thus, for instance, $\langle t_{\epsilon,n}\rangle$ is the mean first-passage time from an ϵ vertex to a site n generations removed. To find these four mean first-passage times for each n we combine the reasoning of Sec. IV of I and that of Sec. III of this paper as follows. First, we define appropriate derivatives of the Laplace transforms of the hopping probability densities evaluated at $s=0$, e.g., [cf. (3.24)],

$$\tilde{p}'_{\epsilon,n} \equiv \left.\frac{d\tilde{p}_{\epsilon,n}(s)}{ds}\right|_{s=0}, \qquad \tilde{q}'_{\omega,n} \equiv \left.\frac{d\tilde{q}_{\omega,n}(s)}{ds}\right|_{s=0}. \tag{4.17}$$

The mean first-passage times of interest are related to these derivatives:

$$\begin{aligned}
\langle t_{\epsilon,n}\rangle &= -\tilde{p}'_{\epsilon,n} - \tilde{q}'_{\epsilon,n} - \tilde{r}'_{\epsilon,n},\\
\langle t_{\omega,n}\rangle &= -\tilde{p}'_{\omega,n} - \tilde{u}'_{\omega,n} - \tilde{r}'_{\omega,n},\\
\langle t_{\beta,n}\rangle &= -\tilde{u}'_{\beta,n},\\
\langle t_{\alpha,n}\rangle &= -\tilde{q}'_{\alpha,n}.
\end{aligned} \tag{4.18}$$

Next, we take derivatives of the renormalization equations themselves to obtain a set of recursion formulas directly for the derivatives of the hopping probability densities [cf. (3.25)]:

$$\begin{pmatrix} \tilde{p}'_{\epsilon,n}\\ \tilde{q}'_{\epsilon,n}\\ \tilde{r}'_{\epsilon,n}\\ \tilde{p}'_{\omega,n}\\ \tilde{u}'_{\omega,n}\\ \tilde{r}'_{\omega,n}\\ \tilde{u}'_{\beta,n}\\ \tilde{q}'_{\alpha,n} \end{pmatrix} = \mathbf{J}_n(0) \begin{pmatrix} \tilde{p}'_{\epsilon,n-1}\\ \tilde{q}'_{\epsilon,n-1}\\ \tilde{r}'_{\epsilon,n-1}\\ \tilde{p}'_{\omega,n-1}\\ \tilde{u}'_{\omega,n-1}\\ \tilde{r}'_{\omega,n-1}\\ \tilde{u}'_{\beta,n-1}\\ \tilde{q}'_{\alpha,n-1} \end{pmatrix}. \tag{4.19}$$

The 8×8 Jacobian coefficient matrix $\mathbf{J}_n(0)$ connecting the nth to the $(n-1)$st set depends only on the hopping probabilities considered in Sec. IV C and can be evaluated explicitly [see Eq. (4.11) in I]. The "initial condition" for the recursion relation is given by

$$\begin{pmatrix} \tilde{p}'_{\epsilon,0}\\ \tilde{q}'_{\epsilon,0}\\ \tilde{r}'_{\epsilon,0}\\ \tilde{p}'_{\omega,0}\\ \tilde{u}'_{\omega,0}\\ \tilde{r}'_{\omega,0}\\ \tilde{u}'_{\beta,0}\\ \tilde{q}'_{\alpha,0} \end{pmatrix} = \begin{pmatrix} -P_{\epsilon,0}/\lambda_\epsilon\\ -Q_{\epsilon,0}/\lambda_\epsilon\\ -R_{\epsilon,0}/\lambda_\epsilon\\ -P_{\omega,0}/\lambda_\omega\\ -U_{\omega,0}/\lambda_\omega\\ -R_{\omega,0}/\lambda_\omega\\ -U_{\beta,0}/\lambda_\beta\\ -Q_{\alpha,0}/\lambda_\alpha \end{pmatrix}, \tag{4.20}$$

where the rates λ_ϵ, λ_ω, λ_β, and λ_α are defined in Eq. (4.5) and the initial hopping probabilities are given in Eqs. (4.6a)–(4.6h).

With enough patience and perseverance the Jacobian matrix can be evaluated and the recursion relation (4.19) with (4.20) solved explicitly as a function of n or, upon rescaling distance and field strength in the usual way, as a function of the product Fx. We have not carried this exercise to completion. Instead, we have concentrated on the weak- and strong-field limits.

For weak fields it can be shown that the above equations reduce to the correct isotropic limit detailed for this system in I. In particular, for the MV model in two dimensions, the mean first-passage time to reach an nth neighbor of any vertex is given by

$$\langle t_n\rangle = 6^n t_0. \tag{4.21}$$

Here t_0 is the mean waiting time for a walker to move to a nearest neighbor on the original structure. In the notation of this section the isotropic case corresponds to $\lambda_\beta=\lambda_\alpha=\lambda_\epsilon/3=\lambda_\omega/3=1/t_0$. We follow the rescaling procedure discussed following Eq. (3.28) and introduce an "effective" hopping rate $\Gamma_n = 1/6^n t_0$, which is independent of the external force. The scaling of this rate that ensures the correct diffusive limit when the external field is vanishingly small is, as in (3.29), given by

$$t_0\Gamma_n = \left(\frac{\Delta x}{x_n}\right)^{d_w} = \left(\frac{\Delta x}{2^n\Delta x}\right)^{d_w}, \tag{4.22}$$

where d_w is the random-walk dimension discussed in I. For the MV model the random-walk dimension is given

by [cf. Eq. (3.15) with $d = 2$ in I]

$$d_w = \frac{\ln 3}{\ln 2} + 1 = 2.58. \tag{4.23}$$

[In other words, we are setting $6^n = (2^n)^{d_w}$.] With this scaling, the mean first-passage time to a site a distance x from any vertex in the weak field limit is given by

$$\langle t(x) \rangle \sim x^{d_w} \sim x^{2.58}. \tag{4.24}$$

Now let us consider the other limiting behavior, namely the strong-field limit. In Appendix C we describe how to obtain the dominant behavior of the mean first-passage time in this limit. The arguments in the appendix lead to the scaling relations

$$\begin{aligned}
\langle t_\alpha(2x,F) \rangle &= e^{\beta F x} \langle t_\alpha(x,F) \rangle, \\
\langle t_\beta(2x,F) \rangle &= e^{-(1-\mu)\beta F x} \langle t_\alpha(x,F) \rangle, \\
\langle t_\epsilon(2x,F) \rangle &= \langle t_\omega(2x,F) \rangle = e^{-(1-\mu)\beta F x} \langle t_\alpha(x,F) \rangle.
\end{aligned} \tag{4.25}$$

We assume a solution of the form

$$\langle t_\alpha(x,F) \rangle = C e^{\beta F x} \tag{4.26}$$

for the longest of the four mean first-passage times. This then finally yields for the mean first-passage time to cover a distance x in the presence of a field and in the limit of a strong field for each of the four vertices

$$\begin{aligned}
\langle t_\alpha(x,F) \rangle &= C e^{\beta F x}, \\
\langle t_\beta(x,F) \rangle &= \frac{C}{\mu} e^{[(\mu+1)/2]\beta F x}, \\
\langle t_\epsilon(x,F) \rangle = \langle t_\omega(x,F) \rangle &= \frac{C}{\mu+1} e^{(1/2)\beta F x}.
\end{aligned} \tag{4.27}$$

The longest time corresponds to exit from a vertex of type α, since the only way out requires the walker to go parallel but opposite to the field. Next is the time to exit vertex β, in a direction at an angle to the field. Finally, the shortest times are those to exit vertices ϵ and ω. These two are equal since their behavior is principally determined by the fact that one pathway involves walking parallel to and along the direction of the field. The other two pathways do not contributed asymptotically to these mean first-passage times.

As the arguments in Appendix C make clear, it would be possible to confirm the assumption (4.26) and it would also be possible to evaluate the constant C analytically if we solved (4.19) with (4.20) completely. Instead, we have evaluated the mean first-passage times numerically as a function of Fx, as shown in Fig. 9. It is clear that these plots of the logarithm of the mean first-passage times as a function of $\beta F x$ rapidly become linear, that is, they confirm the exponential forms (4.27). Using linear regression we obtain, for instance, for $\mu = 1/2$

$$\begin{aligned}
\ln\langle t_\beta(x,F) \rangle &= 1.0044 \beta F x + 36.0977, \\
\ln\langle t_\alpha(x,F) \rangle &= 0.7523 \beta F x + 36.8019, \\
\ln\langle t_\epsilon(x,F) \rangle = \ln\langle t_\omega(x,F) \rangle &= 0.5045 \beta F x + 35.7099.
\end{aligned} \tag{4.28}$$

The calculated slopes agree with those predicted in (4.27)

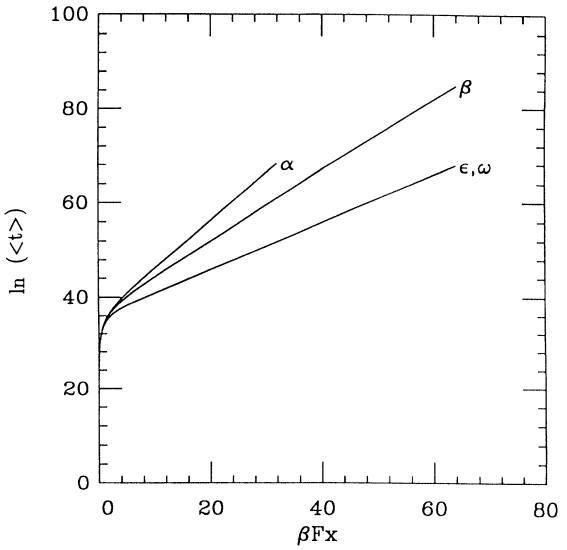

FIG. 9. Mean first-passage time as a function of Fx for the four vertices of the MV model for a branching angle $\theta = \pi/3$ ($\mu = 1/2$).

to within 0.05% [1.0044 for predicted 1; 0.7523 for predicted $(\mu + 1)/2 = 3/4$; 0.5045 for predicted 1/2]. Furthermore, these results confirm the form (4.26) by indeed yielding a common value of the intercept $C = 36$ to within 2%.

V. BIASED WALK ON THE TWO-DIMENSIONAL QUASIRANDOM STRUCTURE

Finally we consider a biased walk on the most general version of our model (albeit restricted to an embedding dimension $d = 2$), i.e., on a quasirandom structure such as the one shown in Fig. 1. The question here is whether the quasirandom character of the structure affects the properties of the walk in a substantial way. If it does, then there is little hope of modeling random structures via deterministic models of the sort that admit analytic solution. If the quasirandom character of the structure does not affect the properties very much, then such modeling is possible—indeed then one can argue that a MV model in particular may represent quite accurately the properties of a biased walk on a DLA.

Again, the field lies parallel to the backbone of the structure and points upward. A walker may begin at any of the six different points shown in Fig. 2 and therefore we must now deal with 12 distinct hopping probabilities. Instead of the four vertices shown in Fig. 6 that had to be considered in the MV model we must now consider 20 different ones. For example, in Fig. 10 we show that what used to be the single vertex 3 in Fig. 6 may now take on eight different configurations as different branches are omitted. Similarly, eight configurations arise from vertex 4, and two each from vertices 1 and 2.

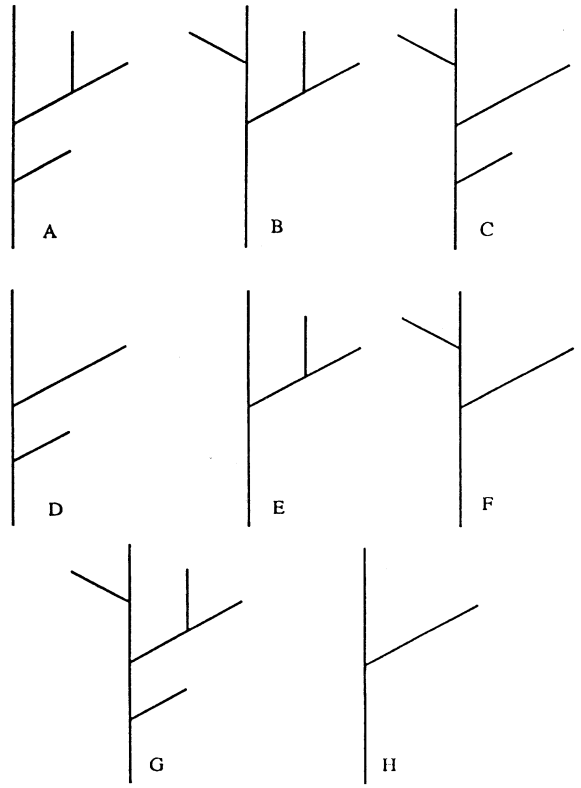

FIG. 10. Eight configurations that arise from vertex 3 in Fig. 7 in the quasirandom model.

The method developed in Sec. IV can clearly be generalized to the present situation. Not only is it necessary to deal with all the possible paths that arise from each of the 20 different configurations, but each one must be weighted according to its probability of occurrence. In the preceding paper I we develop these weightings in detail. For instance, the first configuration in Fig. 10 carries the weight v^3 because each three-unit generator occurs with probability v; the second configuration in the figure carries the weight $v_2(1-v)$ appropriate to two three-unit generators (probability v for each) and a two-unit generator (probability $1-v$).

Little is gained by exhibiting the resulting morass of matrices here. In any case, we did not attempt analytic solutions for the hopping probabilities of this model. Instead, we carried out just a sufficient amount of numerical analysis to verify the dependence or independence of the results on the parameter v since this parameter characterizes the randomness of the structure (the MV model is recovered when $v=1$). Similarly, we did not attempt to solve analytically the 12×12 Jacobian problem for the first-passage times.

The behavior of the system in the weak-field limit is the isotropic behavior detailed in I and need not be repeated here. In this limit there are of course differences between the different structures, and these differences have been captured in the v dependence of the various fractal dimensions.

The limit of interest here is the strong-field limit. Our calculations lead us to conclude that, in the limit of strong fields, walks on quasirandom structures behave essentially the same as on the MV structure, that is, that the principal features of the walk arise from the dead ends in the system where a walker gets trapped for a long time. Indeed, for the hopping probabilities we observe the same maxima associated with steps at an angle to the backbone as seen in Figs. 7 and 8 as a result of the competition among the different directions described in Sec. IV C. The hopping probabilities approach their asymptotic values with the same exponential dependences as for the MV model.

Representative results for the mean first-passage times for the different vertices are shown in Fig. 11. Exponential increases of the mean first-passage times with increasing field and distance are again observed. Furthermore,

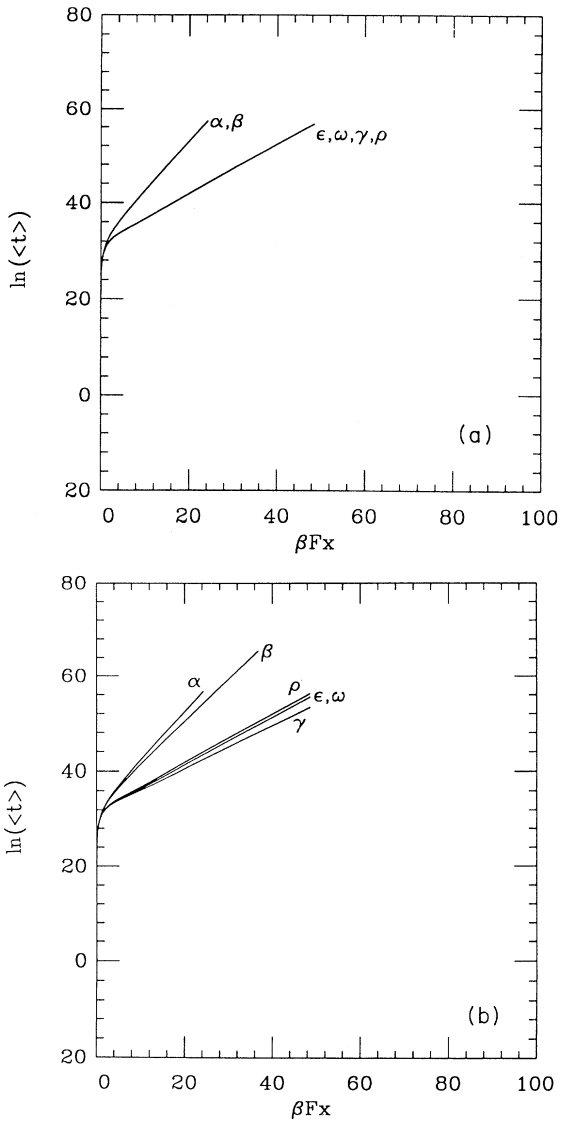

FIG. 11. Mean first-passage times for various vertices in the quasirandom structure and for different branching angles: (a) $\theta=0$; (b) $\theta=\pi/5$.

the coefficients of βFx obtained in these results (that is, the slopes of the logarithm of the mean first-passage times vs Fx) are in complete agreement with those found analytically for the MV model. Thus these coefficients in the exponents are independent of the randomness parameter v. The only place where the randomness has an effect is in the prefactor C of the mean first-passage times [cf. (4.27)]: the prefactor increases as v increases. This is a consequence of the fact that barer structures have shorter mean first-passage times since they have fewer dead ends to trap the walkers.

VI. CONCLUSIONS

We have complemented the analysis of the preceding paper I by considering the effect of an external field of the behavior of a random walker on various fractal structures. In particular, we considered the Mandelbrot-Vicsek structure designed to mimic the behavior of diffusion-limited aggregates, as well as certain quasirandom generalizations of this structure. The field is applied in a direction parallel to the backbone of the structure and in the direction of the branching of the structure (i.e., upwards in all the figures). We have extended the renormalization procedure discussed in I to deal with the anisotropic problem.

For small external fields and/or short distances we recover the results of the isotropic problem. In this limit the hopping probabilities are direction independent and the mean first-passage times to cover a distance x scale as x^{d_w}, where d_w is the random-walk dimension associated with the structure.

For large fields and/or long distances, the walks are dominated by the dead ends from which it is difficult for a walker to leave against the direction of the field. The asymptotic behavior of hopping probabilities and mean first-passage times is exponential in the field and the distance. The hopping probabilities parallel to the backbone grow (upward) and decay (downward) exponentially, and the hopping probabilities in the branching directions have a nonmonotonic behavior that reflects the competition of these branches with the upward motion as downward motion becomes more and more difficult. The associated mean first-passage times grow exponentially, the longest times being those involving walkers that begin from a dead end from which it is necessary to step downward against the field before any other motion is possible.

We find that the behavior of the walker in the large-field limit is entirely dominated by the dead ends and is insensitive to the regularity or randomness of the structure. The transport properties of a structure in this limit are essentially entirely determined by the number of dead ends on the structure. We believe that the same description is valid for random fractals such as the DLA, that is, we expect that a walk on such a structure in the presence of a field is dominated by the dead ends that trap a walker and that transition probabilities and mean first-passage times in such a structure will also exhibit exponential field and distance dependences [15,16].

ACKNOWLEDGMENTS

We gratefully acknowledge support from the U.S. Department of Energy Grant No. DE-FG03-86ER13606 and from Grants No. PB91-0222 and No. PB91-0378 of the Dirección General de Investigación Científica y Técnica (Spain).

APPENDIX A: RENORMALIZATION EQUATIONS FOR THE ONE-DIMENSIONAL BIASED WALK

In this appendix we briefly illustrate the fact that the renormalization equations can be calculated in the same way as was done in I, that is, by explicitly counting paths. In order to calculate the hopping-time distribution for arrival at the next-nearest neighbor 4 in Fig. 3 before arrival at next-nearest neighbor 5 we construct the following relation:

$$\tilde{p}_1(s) = \tilde{p}_0(s)\tilde{p}_0(s) + \tilde{p}_0(s)\tilde{q}_0(s)\tilde{p}_1(s) + \tilde{q}_0(s)\tilde{p}_0(s)\tilde{p}_1(s). \tag{A1}$$

This equation is reasoned as follows: to reach site 4 (before reaching 5) the walker can do one of three things: (i) it can take two steps to the right, as embodied in the first contribution above; (ii) it can take one step to the right, then one to the left back to the origin, and then start all over again (as embodied in the second contribution); or (iii) it can take one step to the left, then one to the right back to the origin, and from there start all over again (third contribution). Solving (A1) for $\tilde{p}_1(s)$ immediately yields (3.7a).

APPENDIX B: MATRICES FOR THE MV MODEL

The four matrices that arise in Eq. (4.1) are given as follows, in terms of the notation introduced in Fig. 2. Each of the matrix elements should carry a subscript 0 and an argument t, both of which we have omitted for economy of notation. In $\mathbf{A}_0^{(1)}$ and $\mathbf{A}_0^{(2)}$ the rows and columns are labeled in the order $(0, 1, 1')$ of Fig. 6, while in $\mathbf{A}_0^{(3)}$ and $\mathbf{A}_0^{(4)}$ they are labeled in the order $(0, 1, 1', 2, 2', 3, 3')$:

$$\mathbf{A}_0^{(1)}(t) = \begin{pmatrix} 0 & q_\alpha & 0 \\ p_\epsilon & 0 & r_\epsilon \\ 0 & u_\beta & 0 \end{pmatrix}, \tag{B1}$$

$$\mathbf{A}_0^{(2)}(t) = \begin{pmatrix} 0 & u_\beta & 0 \\ r_\omega & 0 & p_\omega \\ 0 & q_\alpha & 0 \end{pmatrix}, \tag{B2}$$

$$\mathbf{A}_0^{(3)}(t) = \begin{pmatrix} 0 & p_\epsilon & 0 & r_\epsilon & 0 & q_\epsilon & 0 \\ q_\epsilon & 0 & r_\epsilon & 0 & 0 & 0 & 0 \\ 0 & u_\beta & 0 & 0 & 0 & 0 & 0 \\ u_\omega & 0 & 0 & 0 & p_\omega & 0 & 0 \\ 0 & 0 & 0 & q_\alpha & 0 & 0 & 0 \\ p_\epsilon & 0 & 0 & 0 & 0 & 0 & r_\epsilon \\ 0 & 0 & 0 & 0 & 0 & u_\beta & 0 \end{pmatrix}, \quad \text{(B3)}$$

$$\mathbf{A}_0^{(3)}(t) = \begin{pmatrix} 0 & u_\omega & 0 & p_\omega & 0 & r_\omega & 0 \\ r_\omega & 0 & p_\omega & 0 & 0 & 0 & 0 \\ 0 & p_\alpha & 0 & 0 & 0 & 0 & 0 \\ q_\epsilon & 0 & 0 & 0 & r_\epsilon & 0 & 0 \\ 0 & 0 & 0 & u_\beta & 0 & 0 & 0 \\ u_\omega & 0 & 0 & 0 & 0 & 0 & p_\omega \\ 0 & 0 & 0 & 0 & 0 & q_\alpha & 0 \end{pmatrix}. \quad \text{(B4)}$$

The column vectors $|\nu_{x^{(k)}}(t)\rangle$ are as follows. With $x^{(1)} = q_\alpha$ for arrival at site a of vertex 1 we have (in row form)

$$|\nu_{q_\alpha}(t)\rangle = (0,\ q_{\epsilon,0}(t),\ 0). \quad \text{(B5)}$$

With $x^{(2)} = u_\beta$ for arrival at site a of vertex 2 we have

$$|\nu_{u_\beta}(t)\rangle = (0,\ u_{\omega,0}(t),\ 0). \quad \text{(B6)}$$

With $x^{(3)} = p_\epsilon$ (for arrival at site a of vertex 3), $x^{(3)} = q_\epsilon$ (for arrival at site c of vertex 3), and $x^{(3)} = r_\epsilon$ (for arrival at site b of vertex 3), we have

$$|\nu_{p_\epsilon}(t)\rangle = (0,\ p_{\epsilon,0}(t),\ 0,\ 0,\ 0,\ 0,\ 0), \quad \text{(B7)}$$

$$|\nu_{q_\epsilon}(t)\rangle = (0,\ 0,\ 0,\ 0,\ 0,\ q_{\epsilon,0},\ 0), \quad \text{(B8)}$$

$$|\nu_{r_\epsilon}(t)\rangle = (0,\ 0,\ 0,\ r_{\epsilon,0},\ 0,\ 0,\ 0). \quad \text{(B9)}$$

Finally, with $x^{(4)} = p_\omega$ (for arrival at site b of vertex 4), $x^{(4)} = u_\omega$ (for arrival at site a of vertex 4), and $x^{(4)} = r_\omega$ (for arrival at site c of vertex 4), we have

$$|\nu_{p_\omega}(t)\rangle = (0,\ 0,\ 0,\ p_{\omega,0},\ 0,\ 0,\ 0), \quad \text{(B10)}$$

$$|\nu_{u_\omega}(t)\rangle = (0,\ u_{\omega,0}(t),\ 0,\ 0,\ 0,\ 0,\ 0), \quad \text{(B11)}$$

$$|\nu_{r_\omega}(t)\rangle = (0,\ 0,\ 0,\ 0,\ 0,\ r_{\omega,0},\ 0). \quad \text{(B12)}$$

APPENDIX C: MEAN FIRST-PASSAGE TIMES FOR THE MV MODEL—STRONG FIELDS

In the limit of strong fields the dominant behavior of the mean first-passage times is determined as follows. Using standard methods, the Jacobian matrix $\mathbf{J}_n(0)$ in (4.19) can be diagonalized by a matrix $\mathbf{V}_n$ whose columns are the eigenvectors of the Jacobian matrix. Let us denote the eigenvalues of $\mathbf{J}_n(0)$ as $\lambda_{n,i}$ with $i = 1, \ldots, 8$. We can then exactly rewrite (4.19) as

$$\begin{pmatrix} \tilde{p}'_{\epsilon,n} \\ \tilde{q}'_{\epsilon,n} \\ \tilde{r}'_{\epsilon,n} \\ \tilde{p}'_{\omega,n} \\ \tilde{q}'_{\omega,n} \\ \tilde{r}'_{\omega,n} \\ \tilde{u}'_{\beta,n} \\ \tilde{q}'_{\alpha,n} \end{pmatrix} = \mathbf{V}_n \mathbf{\Lambda}_n \mathbf{V}_n^{-1} \begin{pmatrix} \tilde{p}'_{\epsilon,n-1} \\ \tilde{q}'_{\epsilon,n-1} \\ \tilde{r}'_{\epsilon,n-1} \\ \tilde{p}'_{\omega,n-1} \\ \tilde{q}'_{\omega,n-1} \\ \tilde{r}'_{\omega,n-1} \\ \tilde{u}'_{\beta,n-1} \\ \tilde{q}'_{\alpha,n-1} \end{pmatrix}. \quad \text{(C1)}$$

The matrix $\mathbf{\Lambda}_n$ is diagonal and has the eigenvalues $\lambda_{n,i}$ of the Jacobian matrix along the diagonal.

For large n one of the eight eigenvalues of the Jacobian matrix dominates all the others asymptotically. Let us call this eigenvalue 1, i.e., $\lambda_{n,1}$ is the largest of the eight eigenvalues. If we retain only this eigenvalue and neglect all the others, then one can readily convince oneself that (C1) can asymptotically be written as

$$\begin{pmatrix} \tilde{p}'_{\epsilon,n} \\ \tilde{q}'_{\epsilon,n} \\ \tilde{r}'_{\epsilon,n} \\ \tilde{p}'_{\omega,n} \\ \tilde{q}'_{\omega,n} \\ \tilde{r}'_{\omega,n} \\ \tilde{u}'_{\beta,n} \\ \tilde{q}'_{\alpha,n} \end{pmatrix} = C_n \lambda_{n,1} \begin{pmatrix} v_{n,1} \\ v_{n,2} \\ v_{n,3} \\ v_{n,4} \\ v_{n,5} \\ v_{n,6} \\ v_{n,7} \\ v_{n,8} \end{pmatrix}, \quad \text{(C2)}$$

where the column vector $\mathbf{v}_n$ on the right of the equation is the eigenvector of $\mathbf{V}_n$ associated with the eigenvalue $\lambda_{n,1}$. We have calculated the dominant eigenvalue and associated eigenvector explicitly. In terms of the rescaled variables $F_n x_n \to Fx$ we find

$$\lambda_1(x,F) = e^{\mu\beta Fx} + e^{\beta Fx}, \quad \text{(C3)}$$

$$\mathbf{v}(x,F) = \begin{pmatrix} 1 \\ e^{(1-\mu)\beta Fx} \\ 0 \\ 1 \\ e^{(1-\mu)\beta Fx} \\ 0 \\ \frac{\mu+1}{\mu}(e^{\mu\beta Fx} + e^{\beta Fx}) \\ (\mu+1)(e^{(2-\mu)\beta Fx} - e^{\beta Fx}) \end{pmatrix},$$

where again $\mu < 1$ is the cosine of the angle between the angled branches and the backbone of the structure. The coefficient $C(x,F)$ [common to all the elements of (C2)] can be calculated explicitly from the inverse of $\mathbf{V}(x,F)$. We have not done this (although it is, of course, in principle straightforward to do so). Instead we have evaluated its effect numerically for particular values of μ as described in Sec. IV D.

For large Fx we can simplify these results further by retaining only the leading exponential contributions:

$$\lambda_1(x,F) \sim e^{\beta F x}, \qquad \mathbf{v}(x,F) \sim \begin{pmatrix} 1 \\ e^{(1-\mu)\beta F x} \\ 0 \\ 1 \\ e^{(1-\mu)\beta F x} \\ 0 \\ \frac{\mu+1}{\mu} e^{\beta F x} \\ (\mu+1)e^{(2-\mu)\beta F x} \end{pmatrix}. \tag{C4}$$

For large Fx we thus write (C2) as

$$\mathbf{v}(x,F) = \begin{pmatrix} \tilde{p}'_\epsilon(x,F) \\ \tilde{q}'_\epsilon(x,F) \\ \tilde{r}'_\epsilon(x,F) \\ \tilde{p}'_\omega(x,F) \\ \tilde{q}'_\omega(x,F) \\ \tilde{r}'_\omega(x,F) \\ \tilde{u}'_\beta(x,F) \\ \tilde{q}'_\alpha(x,F) \end{pmatrix}$$

$$= C(x,F)e^{\beta F x} \begin{pmatrix} 1 \\ e^{(1-\mu)\beta F x} \\ 0 \\ 1 \\ e^{(1-\mu)\beta F x} \\ 0 \\ \frac{\mu+1}{\mu} e^{\beta F x} \\ (\mu+1)e^{(2-\mu)\beta F x} \end{pmatrix}. \tag{C5}$$

Finally, for the mean first-passage times of interest (4.18) gives

$$\begin{aligned} \langle t_\epsilon(x,F)\rangle &= -\tilde{p}'_\epsilon(x,F) - \tilde{q}'_\epsilon(x,F) - \tilde{r}'_\epsilon(x,F), \\ \langle t_\omega(x,F)\rangle &= -\tilde{p}'_\omega(x,F) - \tilde{u}'_\omega(x,F) - \tilde{r}'_\omega(x,F), \\ \langle t_\beta(x,F)\rangle &= -\tilde{u}'_\beta(x,F), \\ \langle t_\alpha(x,F)\rangle &= -\tilde{q}'_\alpha(x,F). \end{aligned} \tag{C6}$$

Therefore combining (C5) and (C6) immediately leads to the scaling relations (4.25) in Sec. IV D. In writing these relations we note that the largest component of $\mathbf{v}(x,F)$ is the eigth one, and therefore according to (C6) the longest mean first-passage time is $\langle t_\alpha(x,F)\rangle$. We have chosen to refer all the other mean-first passage times to this one.

* Permanent address: Departamento de Física Aplicada I, Universidad Complutense, 28040 Madrid, Spain.

[1] H. L. Martinez, J. M. R. Parrondo, and K. Lindenberg, preceding paper, Phys. Rev. E **48**, 3545 (1993).

[2] T. A. Witten and L. M. Sanders, Phys. Rev. Lett. **47**, 1400 (1981).

[3] M. Matsushita, M. Sano, Y. Hayakawa, H. Honjo, and Y. Sawada, Phys. Rev. Lett. **53**, 286 (1984); Y. Sawada, A. Dougherty, and J. Gollub, *ibid.* **56**, 1260 (1986); D. Grier E. Ben-Jacob, R. Clarke, and L. Sander, *ibid.* **56**, 1264 (1986).

[4] E. W. Montroll and G. H. Weiss, J. Math. Phys. **6**, 167 (1965); E. W. Montroll and B. J. West, *Fluctuation Phenomena*, edited by E. W. Montroll and J. L. Lebowitz (North-Holland, Amsterdam, 1987).

[5] B. B. Mandelbrot and T. Vicsek, J. Phys. A **22**, L377 (1989).

[6] J. Machta, Phys. Rev. B **24**, 5260 (1981).

[7] C. Van den Broeck, Phys. Rev. Lett. **62**, 1421 (1989); Phys. Rev. A **40**, 7334 (1989); in *Proceedings of the Irreversible Processes and Self-Organization-4 Conference, Rostock, 1989*, edited by W. Ebelbing and H. Ulbricht (Teubner-Texte zur Physik, Leipzig, 1991).

[8] J. M. R. Parrondo, H. L. Martinez, R. Kawai, and K. Lindenberg, Phys. Rev. A **42**, 723 (1990).

[9] C. Van den Broeck and V. Balakrishan, Ber. Bunsenges. Phys. Chem. **95**, 342 (1991).

[10] J. Von Newman and S. M. Ulam, Bull. Am. Math. Soc. **53**, 1120 (1947).

[11] A. S. Glass, K. J. Laidler, and H. Eyring, *The Theory of Rate Processes* (McGraw-Hill, New York, 1941).

[12] R. Ghez, *A Premier of Diffusion Problems* (Wiley, New York, 1988).

[13] S. Havlin and D. ben-Avraham, Adv. Phys. **36**, 695 (1987).

[14] A. Blumen, J. Klafter, and G. Zumofen, *Optical Spectroscopy of Glasses*, edited by I. Zschokke (Reidel, Dordrecht, 1986).

[15] J. K. Kjems, *Fractals and Disordered Systems*, edited by A. Bunde and S. Havlin (Springer-Verlag, Berlin, 1991).

[16] J. P. Bouchard and A. Georges, Phys. Rep. **195**, 127 (1990).